Available online at www.sciencedirect.com
SCIENCE DIRECT®
Journal of Organometallic Chemistry 690 (2005) 874–884
Journal of Organometallic Chemistry
www.elsevier.com/locate/jorganchem

Titanium and zirconium ketimide complexes: synthesis and ethylene polymerisation catalysis

Ana M. Martins [a,*], M. Mercês Marques [a,*], José R. Ascenso [a], Alberto R. Dias [a], M. Teresa Duarte [a], Anabela C. Fernandes [a], Susete Fernandes [a], M. João Ferreira [a], Inês Matos [a], M. Conceição Oliveira [a], Sandra S. Rodrigues [a], Claire Wilson [b]

[a] *Complexo I, Instituto Superior Técnico, Av. Rovisco Pais, 1, 1049-001, Lisboa, Portugal*
[b] *School of Chemistry, University of Nottingham, Nottingham, NG7 2RD, UK*

Received 14 September 2004; accepted 16 October 2004
Available online 24 November 2004

Abstract

The syntheses of ketimide titanium complexes of the type $Ti(N{=}C^tBu_2)_3X$ (X = Cl, Cp, Ind), $Ti(N{=}C^tBu_2)_4$ and the zirconium complex $CpZr(N{=}C^tBu_2)_2Cl$ are described. When activated by MAO, all compounds are ethylene polymerisation catalysts. In the conditions studied, the most active catalyst is $CpZr(N{=}C^tBu_2)_2Cl$, with an activity of 2.7×10^5 kg/(molZr [E] h). Titanium complexes are less active by about two orders of magnitude. The polyethylene produced is linear, as determined by NMR spectroscopy. Molecular structures of $Ti(N{=}C^tBu_2)_3X$ (X = Cl, Cp, Ind) and $Ti(N{=}C^tBu_2)_4$ were determined by X-ray single crystal diffraction.

Keywords: Titanium; Zirconium; Ketimide complexes; Ethylene polymerisation

1. Introduction

The search for non-metallocene olefin polymerisation catalyst has dominated the chemistry of Group 4 metal complexes over the past decades. Carbon-, nitrogen- and oxygen-based ligands have been replacing one or both Cp ligands of metallocenes, giving rise to new classes of compounds that have a wide range of activities towards the polymerisation of olefins [1]. Nitrogen-based ligands have, in particular, been given much attention over the past decade and, as a result, new support moieties for Group 4 complexes, many of which are active catalysts in olefin polymerisation, have been reported [2–12].

Although known for several decades, ketimide ligands never played an important role in early transition metal chemistry. Recently, however, compounds $Cp'Ti(N{=}CR_2)X_2$ were patented by Nova Chemicals [13,14]. These are highly active olefin polymerisation catalysts, with reported activities of 10^8 g/(molTi [E] h) and 10^7 g/(molTi [E] h) for ethylene and propylene homopolymerisation, respectively [15]. $Cp_2Zr(N{=}CR_2)Cl$ was also reported recently [16,17] and tested as an olefin polymerisation catalyst, showing a slightly lower activity than Cp_2ZrCl_2. Ketimide ligands are thus emerging as potential ancillary ligands in Group 4 chemistry.

In this paper, we report the syntheses of a new half-sandwich ketimide Zr(IV) complex and its behaviour in ethylene polymerisation catalysis. We also report the synthesis of new Ti(IV) complexes containing three

* Corresponding authors. Tel.: +351 218419172; fax: +351 218464457 (A.M. Martins), Tel.: +351 218419613; fax: +351 218464457 (M.M. Marques).
E-mail addresses: ana.martins@ist.utl.pt (A.M. Martins), pci011@mail.ist.utl.pt (M.M. Marques).

0022-328X/$ - see front matter © 2004 Elsevier B.V. All rights reserved.
doi:10.1016/j.jorganchem.2004.10.030

and four ketimide ligands and their ethylene polymerisation activity.

2. Results and discussion

2.1. Synthesis and characterization

Treatment of $TiCl_4$ with two equivalents of $LiN{=}C^tBu_2$ in toluene affords $Ti(N{=}C^tBu_2)_3Cl$, **1** (Scheme 1). This non-stoichiometric product is obtained pure as a bright-red microcrystalline solid in the conditions described, in various reaction scales (see Section 3 for details). Changing reaction conditions such as the $TiCl_4$:$LiN{=}C^tBu_2$ ratio or using $TiCl_4(THF)_2$ in THF with 1:2 or 1:3 ratios affords **1**, in similar yields, as the major component of a mixture of compounds that we were unable to identify.

Proton and carbon NMR data for **1** are comparable to other Ti–ketimide complexes found in the literature [15,18,19] Experimental values for elemental analysis are slightly lower than the theoretical ones, probably due to the compound's high sensitivity to air and moisture and so, its formulation was confirmed by high-resolution electron ionisation mass spectrometry (EI/FT ICR-MS). The spectrum shows a signal at m/z = 503.33779 corresponding to $[C_{27}H_{54}N_3Cl^{48}Ti]^-$ with the correct isotopic pattern.

Suitable crystals for X-ray single crystal analysis were grown overnight from a concentrated hexane solution at 4 °C. The molecular structure of **1** is shown in Fig. 1. Selected bond lengths and angles are presented in Table 1. The titanium coordination is best described as distorted tetrahedral, with angles ranging from 105.8(3)° to 113.6(3)°. The ketimide ligands are arranged around

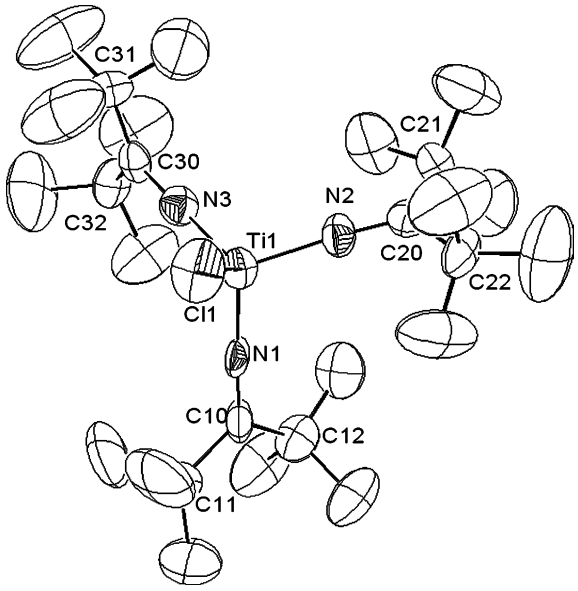

Fig. 1. Molecular structure of **1** showing atom-labeling scheme. Hydrogen atoms are omitted for clarity (thermal ellipsoids at 40% probability level).

the Ti–Cl axis in a propeller-like fashion, with angles between the Ti–Cl axis and the axis defined by the quaternary carbons of the ketimide ligands between 36.06(30)° and 46.02(38)°. The Ti–N=C angles are nearly linear, varying from 170.8(7)° to 175.6(7)°. This is a common feature of Group 4 ketimide complexes [15,16,19] and implies that the N atom has an sp hybridization. The Ti–N bond has therefore some π character, as reflected by the Ti–N distances. The values encountered for this complex (between 1.817(12) and 1.836(8) Å) are typical of titanium–ketimide complexes [15,19] and lay between Ti=NR distances (average of 1.722 Å [20]) and Ti–NR_2

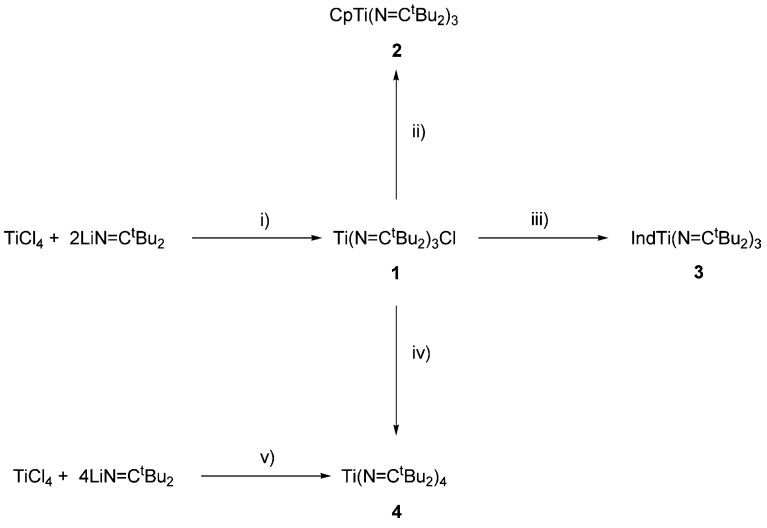

Scheme 1. (i) Toluene, −80 °C to R.T., (ii) NaCp, THF, R.T., (iii) NaInd, THF, R.T., (iv) $LiN{=}C^tBu_2$, toluene, −50 °C to R.T; (i) Toluene, −80 °C to R.T.

Table 1
Selected bond lengths (Å) and angles (°) for compound **1**

Bond lengths (Å)		Angles (°)	
Ti1–N1	1.817(12)	N1–Ti1–N2	109.3(4)
Ti1–N2	1.834(9)	N1–Ti1–N3	107.1(3)
Ti1–N3	1.836(8)	N2–Ti1–N3	105.8(3)
Ti1–Cl1	2.268(4)	N1–Ti1–Cl1	109.7(3)
N1–C10	1.273(12)	N2–Ti1–Cl1	111.0(3)
N2–C20	1.250(11)	N3–Ti1–Cl1	113.6(3)
N3–C30	1.261(11)	C10–N1–Ti1	173.5(7)
		C20–N2–Ti1	170.8(7)
		C30–N3–Ti1	175.6(7)
		C11–C10–C12	123.4(9)
		C21–C20–C22	123.8(8)
		C31–C30–C32	123.8(9)
		(Ti1–Cl1)–(C11–C12)	36.06(30)
		(Ti1–Cl1)–(C21–C22)	46.02(38)
		(Ti1–Cl1)–(C31–C32)	40.81(45)

bond lengths (mean value of 1.939 Å [21]). The N=C bond lengths are similar to those found in reported titanium–ketimide complexes [15,19] and the Ti–Cl distance is also typical of a terminal titanium–chloride bond [21].

Compound **1** reacts with NaCp and NaInd in THF to afford dark orange $CpTi(N{=}C^tBu_2)_3$, **2**, and dark red $IndTi(N{=}C^tBu_2)_3$, **3**, in essentially quantitative yields (Scheme 1). The NMR spectra of **2** and **3** show ^{t}Bu, Cp and Ind at the usual chemical shifts, both in the ^{1}H and the ^{13}C spectra. However, the ^{13}C resonance for the N=C carbon in both compounds is shifted upfield when compared with **1** (180.8 ppm for **2** and 182.2 ppm for **3** vs 197.3 for **1**) or with any other Ti–ketimide complexes found in the literature [15,18,19]. This is consistent with a richer metal centre and thus the imine carbon resonance can be used as a probe for the acidity of titanium–ketimide complexes.

Suitable crystals for X-ray diffraction of complex **2** were obtained in a few hours from a concentrated hexane solution at 4 °C. Compound **3**, which is more soluble, afforded good quality crystals from a hexamethyldisilane concentrated solution, also at 4 °C. Figs. 2 and 3 depict the molecular structures of complexes **2** and **3**, respectively. Selected bonds lengths and angles are presented in Table 2. Complex **3** has two different molecules in the asymmetric unit, with similar structural parameters. Only one is shown. The molecule not shown had disorder in one of the ^{t}Bu groups, which was modelled satisfactorily.

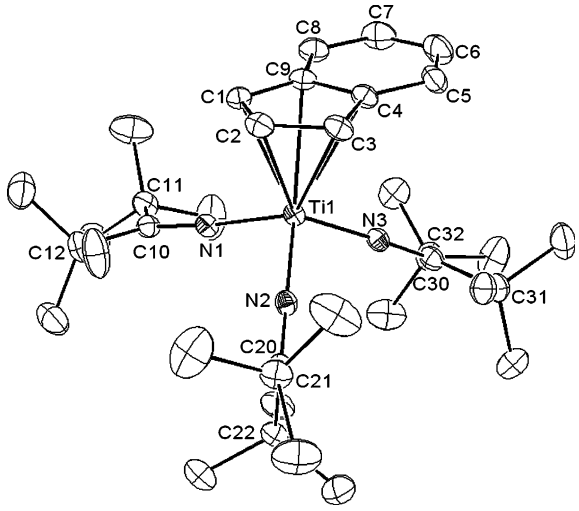

Fig. 3. Molecular structure of **3** showing atom-labeling scheme. Hydrogen atoms are omitted for clarity (thermal ellipsoids at 40% probability level).

Both complexes adopt distorted three-legged piano-stool coordination geometry. The angles of the planes defined by the Cp rings and the planes defined by the three nitrogen atoms are 11.13(0.08) and 9.00(2.50) for complexes **2** and **3**, respectively. The Cp ring in complex **2** is planar (maximum deviation from plane of 0.033(13) Å for C5), with a typical Ti–Cp_{cent} distance of 2.0739(4) Å (Cp_{cent} is the centroid of the C_5 ring) [21]. Likewise, the indenyl ligand is also planar (maximum deviation

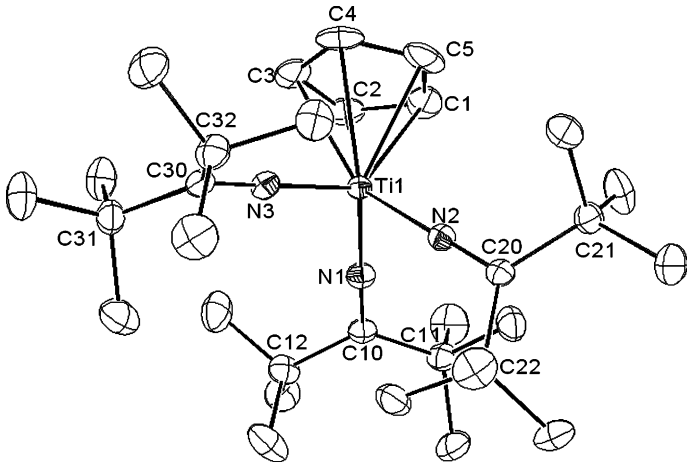

Fig. 2. Molecular structure of **2** showing atom-labeling scheme. Hydrogen atoms are omitted for clarity (thermal ellipsoids at 50% probability level).

Table 2
Selected bond lengths (Å), angles (°) and angles between planes (°) for compounds **2** and **3**

Bond Lengths (Å)	**2**	**3**	Angles (°)	**2**	**3**
Ti1–Cp_{cent}	2.0739(4)	2.1342(4)	Cp_{cent}–Ti1–N1	110.64(6)	108.97(7)
Ti1–N1	1.9082(16)	1.9119(19)	Cp_{cent}–Ti1–N2	128.62(6)	127.28(7)
Ti1–N2	1.8987(15)	1.8865(18)	Cp_{cent}–Ti1–N3	109.50(6)	111.03(7)
Ti1–N3	1.9068(16)	1.9008(18)	N1–Ti1–N2	94.96(7)	95.40(8)
Ti1–C1	2.363(2)	2.396(2)	N1–Ti1–N3	116.31(7)	118.06(8)
Ti1–C2	2.412(2)	2.338(2)	N2–Ti1–N3	96.45(6)	96.06(8)
Ti1–C3	2.431(2)	2.390(2)	Ti1–N1–C10	179.17(15)	172.68(16)
Ti1–C4	2.393(2)	2.564(2)	Ti1–N2–C20	179.15(14)	176.32(16)
Ti1–C5[a]/Ti1–C9[b]	2.356(2)	2.559(2)	Ti1–N3–C30	178.98(15)	176.96(17)
N1–C10	1.259(2)	1.262(3)	C11–C10–C12	122.11(16)	121.93(19)
N2–C20	1.260(2)	1.263(3)	C21–C20–C22	123.88(15)	123.20(18)
N3–C30	1.262(2)	1.260(3)	C31–C30–C32	122.90(16)	122.81(18)
Angles between planes and angles between axis (°)					
Cp_{cent}–(N1–N2–N3)				11.13(8)	9.00 (2.50)
(Cp_{cent})–(C10–C11–C12)				25.70(14)	10.11(32)
(Cp_{cent})–(C20–C21–C22)				89.34(13)	83.96(13)
(Cp_{cent})–(C30–C31–C32)				25.22(22)	34.70(19)
(Cp_{cent}–Ti)–(C11–C12)				81.89(7)	89.46(3.19)
(Cp_{cent}–Ti)–(C21–C22)				38.06(6)	41.25(3.35)
(Cp_{cent}–Ti)–(C31–C32)				89.56(7)	81.17(2.75)

Cp_{cent} is the centroid of the aromatic ring (Cp for **2** and Ind for **3**).
[a] For complex **2**.
[b] For complex **3**.

from plane of 0.0612(373) Å for C2 for all nine atoms). The angle between the planes defined by the five- and the six-carbon rings is only 3.58(15)°. The Cp_{cent}–Ti distance is 2.1343(4) Å.

The distortion in the three-legged piano-stool coordination geometry is best illustrated by the angles around the titanium atom. The Cp_{cent}–Ti–N angles vary from 109.50(6)° to 128.62(6)° for **2**, and from 108.97(7)° to 127.28(7)° for **3**, whereas the N–Ti–N angles vary from 94.96(7)° to 116.31(7)° for **2** and from 95.40(8)° to 118.06(8)° for **3**. This is a direct consequence of the bulkiness of the ketimide ligands. In both complexes, the Cp_{cent}–Ti–N(2) (128.62(6)° for **2** and 127.28(7)° for **3**) and the N(1)–Ti–N(3) (116.31(7)° for **2** and 118.06(8)° for **3**) angles are significantly larger than the other angles around the titanium atoms because there are two ligands positioned roughly parallel to the C_5 plane (angles of 25.70(14)° and 25.22(22)° for **2** and 10.11(32)° and 34.70(19)° for **3**), whereas the third is placed almost vertically (89.34(13)° for **2** and 83.96(13)° for **3**). The propeller-like arrangement of the ketimide ligands found in **1** is thus lost. The angles between the Ti–Cp_{cent} axis and the axis defined by the two ^{t}Bu quaternary carbons of each ketimide ligand vary from 38.06(6)° to 89.56(7)° for **2** and from 41.25(3.35)° to 89.46(3.19)° for **3** (see Table 2). Interestingly, there is only one signal for the ^{t}Bu groups in the ^{1}H NMR spectrum even at −80 °C, implying a fast exchange in the NMR time-scale between the horizontal and the vertical arrangements. The Ti–N bond distances are slightly longer than the analogous bonds in **1**. The values are similar in magnitude to the Ti–NR_2 bonds [22] and reflect the richer metal centres of **2** and **3**, as previously suggested from the NMR data. All other features concerning the ketimide ligands are comparable to **1**.

From the molecular structures above, it is clear that ligands in **2** and **3** offer important steric coverage to the metal centres. This, together with less acidic metal centres, confer unusual robustness to these complexes when compared to other half-sandwich Ti(IV) compounds. Complex **2** survives in contact with air for several days in the solid state and several hours in solution, whereas **3** can survive for a few hours under the same conditions.

Complexes **2** and **3** exhibit ν(N=C) IR frequencies of 1631 and 1626 cm^{-1}, respectively, which are consistent with η^1-ketimide moieties [16].

Ti(N=C^{t}Bu$_2$)$_4$, **4**, was obtained in good yield as a dark red solid both by reaction of **1** with one equivalente of LiN=C^{t}Bu$_2$ and directly by treatment of $TiCl_4$ with four equivalents of LiN=C^{t}Bu$_2$ (Scheme 1). The ^{13}C NMR spectrum of this compound shows the N=C resonance at 188.7 ppm that, compared to **1**, appears up-filed shifted (188.7 vs. 197.3 ppm) as expected for a richer metal centre. This value is, however, down-field shifted relativelly to the correspondent values found in **2** and **3** (188.7 ppm vs. 180.8 ppm for **2** and 182.2 ppm for **3**), consistently with the greater donor ability of the cyclopentadienyl and indenyl rings. This may explain why, unlike **2** and **3**, complex **4** is highly unstable to air and moisture.

Experimental values for elemental analysis are slightly lower than the theoretical ones, probably due to a slight contamination with the crystallization solvent, hexamethyldisilane. The result compares well with a mixture containing 6 molecules of **4** per molecule of hexamethyldisilane. Complex formulation was confirmed by highresolution mass spectrometry, that gave a signal at 608.51365, corresponding to $[C_{36}H_{72}N_4^{48}Ti]^-$.

Crystals of **4** were obtained but showed poor quality for single crystal X-ray diffraction. It was however possible to determine its molecular structure, depicted in Fig. 4. Relevant bonds and angles are presented in Table 3. The geometry around the titanium atom is best described as slightly distorted tetrahedral, with angles around the titanium atom ranging from 107.9(4)° to 110.3(5)°. Both the Ti–N bonds and the Ti–N=C angles are comparable to those found in **1**, varying in this case between 1.848(9) and 1.906(11) Å and between 171.0(8)° and 177.0(10)°, respectively. Thus, unlike for complexes **2** and **3**, where substitution of the chloride ligand by a Cp and Ind rings influences the Ti–N distances, the entry of a fourth ketimide ligand introduces no significant change. All other features concerning the ketimide ligands are comparable to **1**.

$CpZrCl_3 \cdot DME$ reacts with two equivalents of $LiN{=}C^tBu_2$ in toluene to afford $CpZr(N{=}C^tBu_2)_2Cl$, **5**, as a yellow solid, in 91% yield. Similarly to what was observed for compound **1**, the reaction of $CpZrCl_3 \cdot DME$ with one equivalent of $LiN{=}C^tBu_2$ led, not to the expected $CpZr(N{=}C^tBu_2)Cl_2$, but to **5**. Non-stoichiometric reactions appear thus to be a trend in reactions of Group 4 metals with these ligands and, in this respect, they resemble dialkyl amido ligands, which reactivity is very often controlled by stereochemistry with concomitant ligand exchange reactions. The NMR data for **5** are, as expected, comparable to those of **2**, except for the imine carbon resonance that was not detected, even when long relaxation times were used.

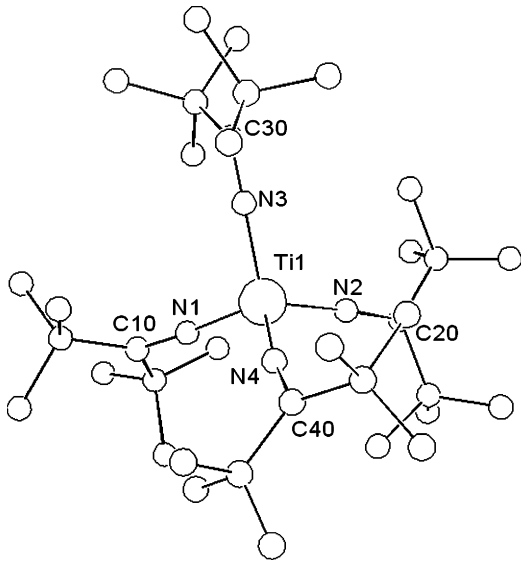

Fig. 4. Molecular structure of **4** showing atom-labeling scheme. Hydrogen atoms are omitted for clarity (thermal ellipsoids at 30% probability level).

Table 3
Selected bond lengths (Å), angles (°) and angles between planes (°) for compound **4**

Bond lengths (Å)		Angles (°)	
Ti1–N1	1.848(9)	N1–Ti1–N2	108.7(4)
Ti1–N2	1.906(11)	N1–Ti1–N3	107.9(4)
Ti1–N3	1.863(8)	N2–Ti1–N3	110.3(5)
Ti1–N4	1.859(9)	N1–Ti1–N4	109.1(4)
N1–C10	1.274(14)	N2–Ti1–N4	105.4(4)
N2–C20	1.272(14)	N3–Ti1–N4	115.2(4)
N3–C30	1.224(16)	C10–N1–Ti1	171.0(8)
N4–C40	1.254(13)	C20–N2–Ti1	177.0(10)
		C30–N3–Ti1	172.1(11)
		C40–N4–Ti1	175.5(8)
		C11–C10–C12	122.4(11)
		C21–C20–C22	124.3(9)
		C31–C30–C32	119.4(12)
		C41–C40–C42	123.3(9)

2.2. Polymerisation studies

The titanium complexes **1**, **2** and **3** were investigated as catalyst precursors in the polymerisation of ethylene. The polymerisation results obtained with the catalysts activated by methylaluminoxane (MAO) are shown in Tables 4–6.

The results indicate that temperature activation is necessary for the polymerisation to occur, since below 40 °C the activity is very low or zero. The maximum in the activity is observed at 80 °C for all the catalyst systems (Table 4). At 98 °C, the activity of **1**/MAO decreases, but it still remains higher than at 60 °C. This effect may be due either to some decomposition of the active species or to the effect of the temperature on the olefin coordination step, since temperature raise increases the rate of olefin dissociation and consequently the falling of active species concentration.

The Al/Ti ratio affects the activity of systems **1**, **2** and **3** that increases with the increase of Al/Ti ratio. The catalyst precursor concentration also affects the activity of all systems. In the case of complexes **1** and **2**, a maximum in activity is reached at the concentration of 160 μM. For complex **3**, the highest activity is observed at the lowest concentration studied, thus revealing an opposite trend (Table 6).

The catalyst systems **1** and **3**/MAO, under the best experimental conditions, show quite similar activities (778 and 1077 kg/(molTi [E] h), respectively). Complex **2**, however, behaves differently. Its activity is around 20 times lower than those of the others. While the activity of the complexes **1** and **3** decreases with the polymer-

Table 4
Ethylene polymerisation by Ti systems (effect of temperature)

Run number	Catalyst	T (° C)	Time (min)	Yield (g)	Activity kg/(molTi [E] h)	T_{max} (°C)	T_{ons} (°C)	ΔH_f (J/g)
PJ2	L_3TiCl, **1**	1	30	0.0048	5.6			
PJ3		21	30	0.0056	7.5			
PJ1		40	30	0.0236	37.8	135.0	124.4	187
PJ5		60	30	0.0488	100.1			
PJ4		80	30	0.2394	702.2	130.5	123.4	223.7
PJ40		98	30	0.1025	506.8			
PJ65		80	60	0.3179	470			
PJ44	L_3TiCp, **2**	1	60	Traces	–			
PJ45		21	60	0.0039	2.5			
PJ43		40	60	0.0195	15.5	137.2	124.8	151.7
PJ46		80	60	0.0313	41.4	132.8	126.5	164.3
PJ101[a]		100	30	0.0330	80.6			
PJ102[a]		100	60	0.0702	94.3			
PJ 75		80	30	0.0085	24.0			
PJ49	L_3TiInd, **3**	1	60	Traces	–			
PJ50		21	60	Traces	–			
PJ48		40	60	0.0303	24.3	136.5	125.2	157.1
PJ52		60	60	0.2081	206.6			
PJ51		80	60	0.2822	400.1	135.9	125.8	178.8
PJ 72		80	30	0.2802	791.1			

Experimental conditions: v = 50 ml toluene; Cocatalyst MAO; Al/Ti = 2000; P(E) = 2 atm; [Ti] = 80 μM except. [a] [Ti] = 160 μM.

Table 5
Ethylene polymerisation by Ti systems (effect of Al/Ti)

Run number	Catalyst	Time (min)	Al/Ti	[Ti] (μM)	Yield (g)	Activity kg/(molTi [E] h)
PJ63	L_3TiCl, **1**	60	500	250	0.3278	155.1
PJ8		30	1000	80	0.0961	276.6
PJ4		30	2000	80	0.2394	702.2
PJ9		30	4000	80	0.2628	756.5
PJ56	L_3TiCp, **2**	60	100	250	–	–
PJ53		60	200	250	0.0132	5.9
PJ54		60	500	250	0.051	22.3
PJ55		60	1000	250	0.1004	44.0
PJ61	L_3TiInd, **3**	60	100	250	0.0006	0.3
PJ58		60	200	250	0.2562	117.9
PJ59		60	500	250	0.3323	149.7
PJ60		60	1000	250	0.5278	235.4

Experimental conditions: v = 50 ml toluene; Cocatalyst MAO; P(E) = 2 atm; T = 80 °C.

isation time, being, after 60 min, around one half of that observed after 30 min (Table 3, runs PJ 4 *vs* PJ 65 and PJ 72 *vs* PJ 51, respectively) the activity of complex **2** increases with the polymerisation time (run PJ 75 *vs* PJ 46 in Table 4). Thus, the results show that under the experimental conditions studied all systems, except **2**/MAO, deactivate along the polymerisation time. The particular behaviour of complex **2** regarding the lower activity observed when compared to that of the other systems for the same reaction times and the increasing of the activity along the polymerisation time may indicate a lower activation rate, related to a higher activation energy. If this is the case, the induction period for this system is longer, leading to lower active species concentration at the initial reaction stage. The raise of concentration of the active species along the polymerisation time would account for the increase of the catalytic activity. The steady increase of the activity with the temperature and with the reaction time even for a temperature of 100 °C, observed for catalyst system **2**/MAO, seams to support this hypothesis. It is possible that for higher polymerisation temperatures the activity pattern of this system becomes similar to that of the other systems studied.

Complex **5** proved to be a very active catalyst in ethylene polymerisation when activated by MAO (see Table 7). Like the titanium compounds, no polymer is obtained at temperatures below 40 °C. The Al/Zr ratio also affects the activity of this system that displays a maximum for an Al/Zr ratio of 2000. The high activity displayed by this system, two to three orders of magnitude higher than the titanium systems studied

Table 6
Ethylene polymerisation by Ti systems. Effect of catalyst concentration

Run number	Catalyst	Time (min)	Al/Ti	[Ti] (μM)	Yield (g)	Activity kg/(molTi [E] h)
PJ37	L_3TiCl, **1**	2000	30	20	0.0421	451.6
PJ38		2000	30	40	0.0994	578.6
PJ4		2000	30	80	0.2394	702.2
PJ39		2000	30	160	0.598	778.1
PJ64		500	60	125	0.2274	224.1
PJ63		500	60	250	0.3278	155.1
PJ75	L_3TiCp, **2**	2000	30	80	0.0085	24.0
PJ76		2000	30	160	0.0196	27.7
PJ57		500	60	125	0.0278	24.0
PJ54		500	60	250	0.051	22.3
PJ74	L_3TiInd, **3**	2000	30	40	0.1909	1077.9
PJ72		2000	30	80	0.2802	791.1
PJ73		2000	30	160	0.4418	623.7
PJ62		500	60	125	0.2786	237.9
PJ59		500	60	250	0.3323	149.7

Experimental conditions: v = 50 ml toluene; Cocatalyst MAO; P(E) = 2 atm; T = 80 °C.

Table 7
Ethylene polymerisation by the Zr system **5**/MAO

Run number	Al/Zr	T °C	Time (min)	[Zr] (μM)	Yield (g)	Activity kg/(molZr [E] h)
101	2000	0	10	20	0	–
102	2000	20	10	20	0	–
100	2000	40	10	20	0.005	28.3
110	2000	60	10	20	0.0758	1681
103	2000	80	10	20	1.2138	31592
109	4000	80	5	5	0.045	11203
106	2000	80	5	5	0.1104	27483
107	1000	80	5	5	0.0157	3257
108	500	80	5	5	0.0180	3754

Experimental conditions: v = 50 ml toluene; Cocatalyst MAO; P(E) = 2 atm.

here, imposed shorter polymerisation times due to diffusion problems in the media. The higher activity of the zirconium system when compared to the titanium ones is in agreement with several results reported in the literature that refer zirconium complexes as much more active than the titanium analogues [23].

^1H and ^{13}C NMR spectra of the polymers show that linear polyethylene was obtained with all the systems. The thermal properties of the polymers were studied by differential scanning calorimetry. The results, included in Table 4, show that an increase in the reaction temperature is always associated with a decrease in the melting temperature, T_{max}, given by the maximum of the melting peak. This may indicate, as expected, that lower molecular weight polymers are obtained at higher polymerisation temperatures. Although the differences in thermal properties of the polymers are small, it is clear that the polymers obtained with the system **1**/MAO have the lowest melting temperature and the highest enthalpy of fusion, independently of the reaction temperature. This result may be attributed to kinetic factors and reflect lower polymer molecular weights. Indeed, lower melting temperatures may be related either to lower polymer crystallinity or to lower polymer molecular weights [24]. Since an increase in crystallinity is observed, a decrease in molecular weights should occur. The highest melting temperatures were observed for polymers obtained with the system **3**/MAO and **2**/MAO at 80 and 40 °C, respectively. The polymer obtained with the zirconium system at 80 °C shows a slightly lower melting temperature (T_m=131.9 °C) and fusion enthalpy (ΔH_f=108.9 J/g) than the polymers obtained with the titanium system.

For the systems described above, the nature of the active species is not yet well established. To get insight into this matter we prepared and performed preliminary catalytic studies with cationic species $[Ti(N{=}C^tBu_2)_3]^+$ [25]. Our results rule out the possibility of olefin insertion into a Ti–N bond and therefore suggest that MAO is responsible not only for the metal alkylation but also for the removal of one ketimide ligand leading to cationic species $[Ti(Me)(N{=}C^tBu_2)_2]^+$. Assuming that a ketimide ligand is also eliminated in systems **2**/-, **3**/- and **5**/MAO, the active species would be $[MCp'(Me)(N{=}C^tBu_2)]^+$. Alternatively, we may envisage the removal of Cp′, which would lead to species

$[M(Me)(N{=}C^tBu_2)_2]^+$. Further studies, aiming to clarify these aspects, are underway [25].

3. Conclusions

Two equivalents of $LiN{=}C^tBu_2$ react with $TiCl_4$ to afford $Ti(N{=}C^tBu_2)_3Cl$, **1**. Chloride substitution by Cp, Ind and $N{=}C^tBu_2$ gives $CpTi(N{=}C\ ^tBu_2)_3$, **2**, $IndTi(N{=}C^tBu_2)_3$, **3**, $Ti(N{=}C^tBu_2)_4$, **4**, respectively, in quantitative yields. Compound **4** was also obtained directly by reaction of $TiCl_4$ with four equivalents of $LiN{=}C\ ^tBu_2$.

Complexes **1**, **2** and **3** are active in the polymerisation of ethylene when activated by MAO, with activities of about 1000 kg/molTi [E] h for all complexes. All titanium complexes show a maximum of activity at 80 °C and an Al/Ti ratio of 2000 provided the best results in all cases. Among all the systems studied, the activation reaction of complex **2** is the slowest one. Not only the catalysts system **2**/MAO shows the lowest activity but also the longest induction period, with continuous activity increases during the first hour of polymerisation reaction.

$CpZrCl_3 \cdot DME$ reacts with two equivalents of $LiN{=}C^tBu_2$ to afford $CpZr(N{=}C^tBu_2)_2Cl$, **5** that is a very active polymerisation catalyst when activated by MAO, with a maximum of activity of 2.7×10^5 kg/(molZr [E] h).

NMR spectra show that the polyethylene produced is linear and DSC experiments show that the thermal parameters are similar for all polymers and that for all systems the increase of the reaction temperature decreases the polymers melting temperature.

4. Experimental

4.1. General procedures

All manipulations, except stated otherwise, were carried out under nitrogen, using either standard Schlenk-line or dry-box techniques.

Solvents were pre-dried using 4 Å molecular sieves and refluxed over sodium-benzophenone (diethyl ether, tetrahydrofuran and toluene) or calcium hydride (dichloromethane, hexamethyldisilane and n-hexane) under an atmosphere of nitrogen, and collected by distillation. Deuterated solvents were dried with molecular sieves and freeze-pump-thaw-degassed prior to use.

^1H and ^{13}C NMR spectra were recorded in a Varian Unity 300, at 298 K, unless stated otherwise. ^1H and ^{13}C NMR spectra were referenced internally to residual protio-solvent (^1H) or solvent (^{13}C) resonances and reported relative to tetramethylsilane (δ 0). Peak assignments were aided by NOE experiments (one-and two-dimensional) and by one bond ^{13}C–^1H hetero-correlations, as appropriate. ^1H NMR and ^{13}C NMR polymer spectra were obtained on samples dissolved in either a mixture of 1,3,5-trichlorobenzene with 30% C_6D_6 at 110 °C (the spectra were referenced internally using hexamethyldisiloxane δ_H 0.058, δ_C 1.9 relative to tetramethylsilane, TMS) or $CDCl_3$ at room temperature.

Infrared spectra were recorded using KBr pellets on a Jasco FT/IR 430. High-resolution electron ionisation (EI) mass spectra were obtained by a Fourier transform ion cyclotron resonance mass spectrometer (Finnegan FT/MS 2001-DT spectrometer), equipped with a 3 Tesla superconducting magnet. Elemental analyses were obtained from the Laboratório de Análises do IST (Fisons Instrument 1108). A differential scanning calorimeter, DSC121 from Setaram, was used to determine the thermal properties of the polymers. In order to minimize the differences in the thermal history of the samples, the polymers were subjected to a heating/cooling/heating cycle, between 30 and 200 °C using a heating rate of 10 °C/min and a cooling rate less than 10 °C/min. After the first heating scan the samples remained at 200 °C for 10 min. The results obtained in the second heating runs were registered and are presented. During the experiments the sample holder was continuously purged with argon.

$TiCl_4$ was purchased from Aldrich and was freeze-pump-thaw-degassed and then distilled trap-to-trap prior to use. MAO (5% Al in toluene) was purchased from Akzo Nobel and used as received. The compounds $LiN{=}C^tBu_2$ [26], NaCp [27], NaInd [27] and $CpZrCl_3 \cdot DME$ [28] were prepared according to literature methods.

4.2. Synthesis of $Ti(N{=}C^tBu_2)_3Cl$ (1)

A suspension of $LiN{=}C^tBu_2$ (5.43 g, 36.9 mmol) in 50 mL of toluene was added to a solution of $TiCl_4$ (3.50 g, 18.5 mmol) in 400 mL of toluene cooled to −80 °C. The reaction mixture turned red immediately. It was allowed to come slowly to room temperature over a period of 3 h and was left stirring at room temperature for 1.5 h. The solvent was pumped-off and the residue extracted with hexane. Solvent removal gave 3.82 g of **1** (41% yield based on Ti) as a bright red microcrystalline solid. ^1H NMR (C_6D_6, 300 MHz): δ 1.27 (s, 54H, ^{t}Bu). ^{13}C NMR (C_6D_6, 75 MHz): δ 197.3 (N=*C*), 45.7 (*C*$(CH_3)_3$), 30.8 (*C*$_3$). EI/FT ICR-MS: 503.33779 (100) ($[C_{27}H_{54}\ N_3Cl^{48}Ti]^-$). Anal. Found (Calc.): C, 62.85 (64.34); H, 10.71 (10.80); N, 7.91 (8.34).

4.3. Synthesis of $CpTi(N{=}C^tBu_2)_3$ (2)

Complex **1** (0.560 g, 1.19 mmol) was dissolved in approximately 10 mL of THF and a solution of NaCp

(0.115 g, 1.31 mmol) in 20 mL of THF was added. The mixture was allowed to stir at room temperature for 24 h. The solvent was pumped-off and the residue was extracted in hexane. Solvent removal affords 0.630 g (99.2% yield) of a dark orange microcrystalline powder. ^{1}H NMR (C_6D_6, 300 MHz): δ 6.05 (s, 5H, Cp), 1.23 (s, 54H, ^{t}Bu). ^{13}C NMR (C_6D_6, 75 MHz): δ 180.8 (*C*=N), 109.8 (Cp), 43.4 (*C*(CH_3)$_3$), 31.1(*C*$_3$). IR ν(N=C) = 1631 cm^{-1}. Anal. Found (Calc.): C, 72.26 (72.02); H, 12.54 (11.14); N, 7.72 (7.87).

4.4. Synthesis of IndTi(N=C^{t}Bu$_2$)$_3$ (3)

To a solution of **1** (0.606 g, 1.20 mmol) in 30 mL of THF, NaInd (0.182 g, 1.32 mmol) in 10 mL of THF was added. The mixture stirred at room temperature for 24 h and the THF was pumped-off. Extraction with hexane affords 0.649 g of a dark-red solid (92.6 % yield). ^{1}H NMR (C_6D_6, 300 MHz): δ 7.48 (dd, $^3J_{H5H6}$ = 6.7 Hz, $^4J_{H5H7}$ = 3.0 Hz, 2H, H5/H8), 6.96 (dd, $^3J_{H5H6}$ = 6.7 Hz, $^4J_{H5H7}$ = 3.0 Hz, 2H, H6/H7), 6.42 (t, $^3J_{H1H2}$ = 3.6 Hz, 1H/H2), 6.32 (d, $^3J_{H1H2}$ = 3.6 Hz, 2H, H1/H3), 1.19 (s, 54H, ^{t}Bu). ^{13}C NMR (C_6D_6, 75 MHz): δ 182.2 (*C*=N), 125.6 (C4/C9), 124.3 (C5/C8), 123.5 (C6/C7), 114.9 (C2), 100.5 (C1/C3), 43.9 (*C* (CH_3)$_3$), 31.2 (C(*C*$_{33}$)). IR ν(N=C) = 1626 cm^{-1}. Anal. Found (Calc.): C, 73.38 (74.07); H, 11.08 (10.53); N, 7.17 (7.20).

4.5. Synthesis of Ti(N=C^{t}Bu$_2$)$_4$ (4)

Method A: A suspension of LiN=C^{t}Bu$_2$ (1.455 g, 9.88 mmol) in 30 mL of toluene was added to a solution of $TiCl_4$ (0.469 g, 2.47 mmol) in 30 mL of toluene, cooled to −50 °C. The temperature was allowed to rise to room temperature for 15 hours. Removal of the solvent and subsequent extraction with hexane afforded 1.340 g (97% yield) of a dark red solid. Method B: LiN=C^{t}Bu$_2$ (0.0962 g, 0.65 mmol) was suspended in 20 mL of toluene and was added to a solution of **1** (0.331 g, 0.66 mmol) in toluene, cooled to −50 °C. The mixture was allowed to reach room temperature over a period of 15 hours and the solvent was then removed. Extraction with hexane afforded 0.376 g of **4** (94% yield). ^{1}H NMR (C_6D_6, 300 MHz): 1.34 (s, 72H, ^{t}Bu). ^{13}C NMR (C_6D_6, 75 MHz): 188.7 (*C*=N), 44.7 (*C*(CH_3)$_3$), 31.2 (*C*$_3$). EI/FT ICR-MS: 608.51365 (100) ([$C_{36}H_{72}N_4^{48}Ti$]$^-$). Anal. Exp. (Calc.): C, 70.25 (70.18); H, 11.82 (11.94); N, 8.86 (8.85).

4.6. Synthesis of CpZr(N=C^{t}Bu$_2$)$_2$Cl (5)

A suspension of LiN=C^{t}Bu$_2$ (0.61 g, 4.14 mmol) in toluene (20 mL) was added dropwise, at −64 °C, to a suspension of $CpZrCl_3$. DME (0.73 g, 2.07 mmol) in the same solvent (20 mL). The solution temperature was allowed to rise to 0 °C during 3 hours, while the colour of the mixture turned orange-yellow. The solvent was pumped off and the residue was extracted in hexane. The yellow solution obtained was separated from the LiCl precipitate by filtration. Removal of the solvent to dryness led to **5** as a yellow crystalline powder, in 91% yield (0.84 g). ^{1}H NMR (C_7D_8, 300 MHz): δ 6.23 (s, 5H, Cp), 1.24 (s, 36H, ^{t}Bu). ^{13}C NMR (C_7D_8, 75 MHz): δ 110.0 (Cp), 43.9 (C(CH_3)$_3$), 31.1 (CH_3). MS (EI, *m*/*z*): 447 (M^+), 412 ({M − Cl}$^+$), 390 ({M − ^{t}Bu}$^+$), 382 ({M − Cp}$^+$), 355 ({M − Cl-^{t}Bu}$^+$), 191 ({ZrCpCl}$^+$), 91 (Zr^+), 65 (Cp^+). Anal. Found (Calc.): C, 58.50 (58.22), H, 8.75 (8.69); N, 5.93 (5.86).

4.7. General procedure for olefin polymerisation

The polymerisation apparatus and polymer work up were described in previous papers [29–31] The polymerisation mixture was quenched with acidic methanol (2%HCl) and the precipitated polymer was filtered, washed with methanol and dried in a vacuum oven at 60 °C during three days.

4.8. General procedure for X-ray crystallography

Pertinent details for the individual compounds can be found in Table 8. Suitable crystals of complex **1** were mounted on a MACH3 Nonius diffractometer equipped with Mo radiation (λ = 0.70169 Å). Data were collected at room temperature. Solution and refinement were made using SIR 97 [32] and SHELXL-97 [33] included in the package of programs WINGX-version 1.64.05 [34]. All non-hydrogen atoms were refined anisotropically and the hydrogen atoms were inserted in idealized positions riding in the parent C atom.

Crystallographic data for complexes **2**, **3** and **4** were collected using graphite monochromated Mo K_α(λ = 0.71073Å) on a Bruker APEX CCD area detector diffractometer equipped with an Oxford Cryosystems open-flow nitrogen cryostat at 150 K. Data were corrected for absorption using a multi-scan method (program SADABS). The structures were solved by direct methods using SHELXS-97 [35] and refined using full-matrix least squares refinement against F^2 using SHELXL-97 [33]. All non-H atoms were refined with anisotropic atomic displacement parameters and hydrogen atoms placed in geometrically calculated positions and included as part of a riding model, except the methyl hydrogen atoms in the structure of complex **3**, which were located from difference Fourier syntheses and refined as a rigid rotor. One ^{t}Bu group in complex **3** showed disorder and was modelled over two half occupied sites. Crystals of complex **4** had very poor diffracting quality, which is shown not only by the weak diffraction pattern, but also by the high thermal parameters, some disorder and finally by the high *R* values. Data was merged for 2/m Laue symmetry and refined in the centrosymmetric space

Table 8
Crystallographic Data for **1**, **2**, **3** and **4**

Compound	**1**	**2**	**3**	**4**
Empirical formula	$C_{54}H_{108}Cl_2N_6Ti_2$	$C_{128}H_{236}N_{12}Ti_4$	$C_{288}H_{488}N_{24}Ti_8$	$C_{432}H_{864}N_{48}Ti_{12}$
Formula weight	504.08	533.72	583.78	913.31
Temperature (K)	293(2)	150(2)	150(2)	150(2)
Wavelength (Å)	0.70169	0.70173	0.70173	0.70173
Crystal system	Triclinic	Monoclinic	Monoclinic	Monoclinic
Space group	$P\bar{1}$	$P121/c1$	$P121/n1$	$C12/c1$
a (Å)	10.274(7)	11.6262(8)	16.5517(11)	32.747(5)
b (Å)	12.146(11)	28.342(2)	11.6032(7)	32.983(5)
c (Å)	13.65(8)	11.2092(7)	37.345(2)	11.9713(17)
α (°)	82.42(6)	90.00	90.00	90.00
β (°)	86.94(5)	116.9180(10)	98.820(1)	108.116(20)
γ (°)	71.48(6)	90.00	90.00	90.00
V (Å^3)	1601(10)	3293.4(4)	7087.4(7)	12289.06(90)
Z	2	4	8	8
D_c (g cm^{-3})	1.046	1.076	1.094	0.987
Absortion coefficient	0.367	0.282	0.268	0.234
$F(0\,0\,0)$	552	1176	2560	4056
Crystal size	$0.52 \times 0.09 \times 0.03$	$0.57 \times 0.49 \times 0.39$	$0.69 \times 0.49 \times 0.06$	$0.66 \times 0.49 \times 0.29$
Crystal morphology	Needle	Block	Tablet	Block
Color	Red	Red	Red	Red
θ range for data collection	1.78° −24.97°	2.09° −27.49°	2.15° −25.01°	1.96° −25.01°
Limiting indices	$0 \leqslant h \leqslant 12$; $-13 \leqslant k \leqslant 14$; $-16 \leqslant l \leqslant 16$	$-15 \leqslant h \leqslant 13$; $0 \leqslant k \leqslant 36$; $0 \leqslant l \leqslant 14$	$-19 \leqslant h \leqslant 19$; $-13 \leqslant k \leqslant 13$; $-43 \leqslant l \leqslant 40$	$0 \leqslant h \leqslant 38$; $0 \leqslant k \leqslant 39$; $-14 \leqslant l \leqslant 14$
Reflections collected/unique	5869/5527 [R_{int} = 0.1474]	7492/7492 [R_{int} = 0.0000]	12,347/12,347 [R_{int} = 0.0000]	10,818/10,818 [R_{int} = 0.0000]
Completeness to theta	98.2% (θ = 24.97°)	99.0% (θ = 27.49°)	98.9% (θ = 25.01°)	99.8% (θ = 25.01)
Refinement method	Full matrix least-squares on F^2	Full matrix least-squares on F^2	Full matrix least-squares on F^2	Full matrix least-squares on F^2
Data/restrains/parameters	5527/0/290	7492/15/343	12,347/36/787	10,818/20/556
Goodness of fit on F^2	0.899	1.248	0.971	2.049
Final R indices [$I > 2\sigma(I)$]	R_1 = 0.1072, wR_2 = 0.2452	R_1 = 0.0551, wR_2 = 0.1230	R_1 = 0.0463, wR_2 = 0.1100	R_1 = 0.1994, $wR2$ = 0.4924
R indices (all data)	R_1 = 0.2415, wR_2 = 0.3072	R_1 = 0.0573, wR_2 = 0.1243	R_1 = 0.0785, wR_2 = 0.1246	R_1 = 0.2220, wR_2 = 0.5065
Extinction coefficient	0.00713	0	0	0
Largest difference peak and hole (e Å^{-3})	−0.603 and 0.540	−0.391 and 0.412	−0.227 and 0.06	1.472 and −1.065

group $C2/c$ with one and half molecule in the asymmetric unit. Nevertheless, the refinement shows undoubtly that complex **4** is present as described. The molecular structures were done with ORTEP3 for Windows [36] included in the software package.

Acknowledgments

The authors thank Fundação para a Ciência e Tecnologia for financial support (projects POCTI/QUI/29734/2001 and POCTI/32771/QUI/2000). M.J.F., I.M., S.F. and S.S.R. are thankful for their scholarships (BD2869/2000, BD10338/2002, BD21354/99 and BPD5541/2001, respectively) by the same institution and FSE. We are grateful to Borealis for the polymerisation equipment.

Appendix A. Supplementary data

Crystal data for complexes **1**, **2, 3** and **4** was deposited at the Cambridge Structural Database (CCDC 242495, CCDC 242496, CCDC 242497 and CCDC 249964, respectively). Copies of this information may be obtained free of charge on application to CCDC, 12 Union Road, Cambridge CB2 1ET, UK. [fax: +44-1223-336033, E-mail: deposit@ccdc.cam.ac.uk]. Supplementary data associated with this article can be found, in the online version at doi:10.1016/j.jorganchem.2004.10.030.

References

[1] V.C. Gibson, S.K. Spitzmesser, Chem. Rev. 103 (2003) 283.
[2] J.R. Ascenso, C.G. Azevedo, M.J. Correia, A.R. Dias, M.T. Duarte, J.L. Ferreira da Silva, P.T. Gomes, F. Lourenço, A.M. Martins, S.S. Rodrigues, J. Organomet. Chem. 632 (2001) 58.
[3] D.A. Kissounko, J.C. Fettinger, L.R. Sita, Inorg. Chim. Acta 345 (2003) 121.
[4] L. Bourget-Merle, M.F. Lappert, J.R. Severne, Chem. Rev. 102 (2002) 3031.
[5] X. Gao, P.S. Chisholm, G. Kowalchuk, R.D. Donaldson, Catalyst for olefin polymerization. Nova Chemicals (International), S.A. 10/074,662 [US 2003/0087754 A1], 2003.
[6] S.J. Brown, X. Gao, D.G. Harrison, I. McKay, L. Koch, Q. Wang, W. Xu, R.E.v.H. Spence, D.W. Stephan, Bis-phosphinimine catalyst. Nova Chemicals (International), S.A. 09/753,387 [US 2001/0007895 A1], 2001.
[7] S.J. Brown, X. Gao, Q. Wang, P. Zoricak, R.E.H. Spence, W. Xu, Phosphinimine/heteroatom catalyst component. Nova Chemicals (International), S.A. 09/328,731 [US 6,147,172], 2000.
[8] P. Mehrkhodavandi, R.R. Schrock, J. Am. Chem. Soc. 123 (2001) 10746.
[9] A. Shafir, J. Arnold, J. Am. Chem. Soc. 123 (2001) 9212.
[10] C. Averbuj, E. Tish, M.S. Eisen, J. Am. Chem. Soc. 120 (1998) 8640.
[11] J.T. Patton, M.M. Bokota, K.A. Abboud, Organometallics 21 (2002) 2145.
[12] R. Vollmerhaus, M. Rahim, R. Tomaszewski, S. Xin, N.J. Taylor, S. Collins, Organometallics 19 (2000) 2161.
[13] J. McMeeking, X. Gao, R.E.V.H. Spence, S.J. Brown, D. Jeremic, Catalyst having a ketimide ligand. Nova Chemicals (International), S.A. [WO 99/14250], 1999.
[14] Q. Wang, P. Lam, Vinylaromatic and olefin pseudoblock polymers. Nova Chemicals (International), S.A. [WO 01/14440 A1], 2000.
[15] A.R. Dias, M.T. Duarte, A.C. Fernandes, S. Fernandes, M.M. Marques, A.M. Martins, J.F. da Silva, S.S. Rodrigues, J. Organomet. Chem. 689 (2004) 203.
[16] D.R. Armstrong, K.W. Henderson, I. Little, C. Jenny, A.R. Kennedy, A.E. McKeown, R.E. Mulvey, Organometallics 19 (2000) 4369.
[17] K.W. Henderson, A. Hind, A.R. Kennedy, A.E. McKeown, R.E. Mulvey, J. Organomet. Chem. 656 (2002) 63.
[18] S. Zhang, W.E. Piers, Organometallics 20 (2001) 2088.
[19] S. Zhang, W.E. Piers, X. Gao, M. Parvez, J. Am. Chem. Soc. 122 (2000) 5499.
[20] Cambridge Structural Database.
[21] A.G. Orpen, L. Brammer, F.H. Allen, O. Kennard, D.G. Watson, R. Taylor, J. Chem. Soc., Dalton Trans. (1989) S1.
[22] A.M. Martins, J.R. Ascenso, C.G. Azevedo, M.J. Calhorda, A.R. Dias, S.S. Rodrigues, L. Toupet, P. de Leonardis, L.F. Veiros, J. Chem. Soc., Dalton Trans. (2000) 4332.
[23] L. Resconi, L. Cavallo, A. Fait, F. Piemontesi, Chem. Rev. 100 (2000) 1253.
[24] T. Trankner, M. Hendeqvist, U.W. Gedde, Polym. Eng. Sci. 34 (1994) 1581.
[25] A.M. Martins, M.M. Marques, M.J. Ferreira, I. Matos, Manuscript in preparation.
[26] W. Clegg, R. Snaith, H.M.M. Shearer, K. Wade, G. Whitehead, J. Chem. Soc., Dalton Trans. (1983) 1309.
[27] W.A. Herrmann, A. Salzer, Literature, laboratory techniques and common starting materials, Thieme, 1996.
[28] E.C. Lund, T. Livinghouse, Organometallics 9 (1990) 2426.
[29] J.C.W. Chien, B.-P. Wang, J. Polym. Sci. Part A: Polym. Chem. 26 (1988) 3089.
[30] M.M. Marques, S.G. Correia, J.R. Ascenso, A.F.G. Ribeiro, P.T. Gomes, A.R. Dias, P. Foster, M.D. Rausch, J.C.W. Chien, J. Polym. Sci. Part A: Polym. Chem. 37 (1999) 2457.
[31] S.G. Correia, M.M. Marques, J.R. Ascenso, A.F.G. Ribeiro, P.T. Gomes, A.R. Dias, M. Blais, M.D. Rausch, J.C.W. Chien, J. Polym. Sci. Part A: Polym. Chem. 37 (1999) 2471.
[32] A. Altomare, M.C. Burla, M. Camalli, G.L. Cascarano, C. Giacovazzo, A. Guagliardi, A.G.G. Moliterni, G. Polidori, R. Spagna, J. Appl. Crystallogr. 32 (1999) 115.
[33] G.M. Sheldrick. SHELXL-97, A Computer Program for Refinement of Crystal Structures, University of Göttigen, 1997.
[34] L.J. Farrugia, J. Appl. Crystallogr. 32 (1999) 837.
[35] G.M. Sheldrick, Acta Crystallogr., Sect. A 46 (1990) 467.
[36] L.J. Farrugia, J. Appl. Crystallogr. 30 (1997) 565.